Accepted Manuscript

Novel tetranuclear ruthenium(II) arene complexes showing potent cytotoxic and antimetastatic activity as well as low toxicity *in vivo*

Mohamed Kasim Mohamed Subarkhan, Lulu Ren, Binbin Xie, Chao Chen, Yuchen Wang, Hangxiang Wang

PII: S0223-5234(19)30588-4

DOI: https://doi.org/10.1016/j.ejmech.2019.06.061

Reference: EJMECH 11464

To appear in: *European Journal of Medicinal Chemistry*

Received Date: 8 March 2019

Revised Date: 19 June 2019

Accepted Date: 21 June 2019

Please cite this article as: M.K. Mohamed Subarkhan, L. Ren, B. Xie, C. Chen, Y. Wang, H. Wang, Novel tetranuclear ruthenium(II) arene complexes showing potent cytotoxic and antimetastatic activity as well as low toxicity *in vivo*, *European Journal of Medicinal Chemistry* (2019), doi: https://doi.org/10.1016/j.ejmech.2019.06.061.

Novel tetranuclear ruthenium(II) arene complexes showing potent cytotoxic and antimetastatic activity as well as low toxicity *in vivo*

*Mohamed Kasim Mohamed Subarkhan,[a] Lulu Ren,[b] Binbin Xie,[b] Chao Chen,[c] Yuchen Wang,[a] and Hangxiang Wang[a,]**

[a] *The First Affiliated Hospital; Key Laboratory of Combined Multi-Organ Transplantation, Ministry of Public Health, School of Medicine, Zhejiang University, Hangzhou, 310003, PR China.*

[b] *Department of Medical Oncology; Sir Run Run Shaw Hospital; School of Medicine, Zhejiang University, Hangzhou, 310016, PR China.*

[c] *College of Life Sciences, Huzhou University, Huzhou, 313000, PR China.*

Corresponding Author: *Hangxiang Wang, The First Affiliated Hospital, School of Medicine, Zhejiang University; 79, Qingchun Road, Hangzhou, 310003, China. Phone: +86-571-88208173; Fax: +86-571-88208173; E-mail: wanghx@zju.edu.cn*

ABSTRACT

Ruthenium complexes have attracted a surge of interest as anticancer drug candidates because of their low toxicity, diversity in mode-of-actions and non-cross drug resistance with conventional platinum-based agents. Despite remarkable advances, only a limited number of ruthenium complexes have been demonstrated to kill cancer cells and suppress metastasis simultaneously. Here, two organometallic tetranuclear Ru(II) arene complexes (**Ru-1** and **Ru-2**) have been synthesized and evaluated for their *in vitro* activity against a panel of human cancer cell lines, including a cisplatin-resistant human lung cancer A549 cell line. A superior cytotoxic activity of the ruthenium complexes compared to cisplatin across distinct cell lines was observed. Further examination of the mechanism indicated that anticancer activity was accomplished by inducing apoptosis in cancer cells. In addition, we found that such compounds exhibited promising antimetastatic activity and reduced the invasiveness of cancer cells. Importantly, choosing **Ru-1** as a target compound, a significantly enhanced safety profile relative to cisplatin in animals was validated, suggesting that these complexes can be used as promising candidates for cancer therapy and deserve further investigation.

KEYWORDS:

tetranuclear Ru(II) arene complexes, *in vitro* cytotoxicity, apoptosis, antimetastasis, drug toxicity

1. INTRODUCTION

Since the first discovery of cisplatin in the 1960s [1], platinum agents have been extensively used as standard-of-care drugs to clinically treat a variety of types of cancer [2]. However, severe side effects (e.g., nephrotoxicity and myelosuppression) and intrinsic or acquired resistance of using these platinum agents have significantly impeded the therapeutic benefits. Consequently, there is a considerable incentive for the exploration of novel non-platinum anticancer agents over the past decades [3-5]. In line with this consideration, a number of metallodrugs have been synthesized and evaluated in preclinical animal models, and some of them have entered different stages of clinical trials [6, 7]. However, despite remarkable advances, none of metallodrugs have been developed as successfully as platinum drugs.

Ruthenium complexes have attracted considerable interest as alternative chemotherapeutics to platinum-based agents. Currently, several ruthenium compounds, such as [Na]*trans*-[Ru(*N*-ind)$_2$Cl$_4$] (NKP1339) and [imiH]*trans*-[Ru(*N*-imi)(*S*-dmso)Cl$_4$] (NAMI-A), have entered phase II clinical trials [8]. For instance, NAMI-A shows negligible cytotoxicity toward tumor cells but is efficient against tumor metastasis and angiogenesis. On the other hand, during the last decade, ruthenium(II) (Ru(II)) arene complexes have been particularly interesting as anticancer drug candidates, presumably due to their chemical properties, air stability, aqueous solubility, and structural diversity [9]. The arene ligands are able to coordinate with the Ru(II) metals strongly, thereby making the overall complexes inert toward substitutions and stabilizing Ru(II) ions in a low oxidation state [10-13]. Thus, arene coordination can confer complexes with enhanced hydrophobicity compared with other types of Ru(II) complexes, thereby altering cellular uptake. In addition, the remaining three ruthenium coordination sites can be occupied with other ligands, readily forming a "*piano-stool*" geometry, which is typical for Ru(II) arene complexes [14-16]. These types of "*piano-stool*" anticancer complexes have been demonstrated to show enhanced cellular uptake and interact with intracellular targets specifically [12]. Prior studies also indicated that Ru(II) complexes bearing a π-conjugated arene ligand and various mono- or bidentate ligands with distinct donor atoms, including N-S [17], N-O [18], N-N [19], N-P [20], O-O [21], P-P [22] [21], and NHC[23], are regarded as cytotoxic drug candidates without exhibiting antimetastatic activity. Therefore, ruthenium complexes that have the ability to simultaneously kill cancer cells and suppress metastasis are promising drug candidates for the management of

metastatic cancers from a clinical perspective.

In the continuing effort to develop Ru(II) complexes, we designed novel tetranuclear Ru(II) arene complexes bearing aroylhydrazone ligands and explored them as efficaciously cytotoxic and antimetastatic agents against cancer cell lines. Our molecular design is based on hydrazone motifs. Hydrazone and its analogs are a class of the most vital natural products, showing biological activities including anticancer properties [24]. Moreover, hydrazone exerts anticancer activity *via* different modes of action, such as kinase inhibition, telomerase inhibition, and cell cycle arrest [25, 26]. These unique functions make hydrazones attractive motifs for the creation of therapeutic ruthenium complexes [27]. Ru(II) complexes have been broadly examined either as single anticancer agents or in combination with other cytotoxic agents; therefore, hybridization of arene Ru(II) with other bioactive pharmacophores is an effective strategy to design novel anticancer agents.

The development of multinuclear metal complexes is also of considerable interest as drug candidates for anticancer treatment [28]. For example, BBR3464 [29], a trinuclear cisplatin compound, is 2-3 orders of magnitude more active than cisplatin in cisplatin-resistant cell lines. However, this agent did not show significant clinical activity in phase II trials [30], suggesting further structural optimization are needed. Despite these advancements, multinuclear Ru(II) arene complexes are scarcely explored as anticancer agents to date [31]. Herein, we rationally incorporated a hydrazone moiety into tetranuclear Ru(II) arene complexes to improve the pharmacological activity. To test this rationale, two tetranuclear arene Ru(II) hydrazone complexes (i.e., **Ru-1** and **Ru-2**) were designed, and the anticancer activity was evaluated. The *in vitro* cell-based results supported the high potency of using our Ru(II) complexes to induce cell death against a small panel of cancer cell lines, including a cisplatin-resistant human lung cancer A549 cell line. More interestingly, the **Ru-1** complex was able to inhibit the migration and invasion of cancer cells. Finally, the *in vivo* toxicity studies clearly demonstrated that **Ru-1** possessed higher safety margins in animals compared to the cisplatin agent, warranting further investigation.

2. RESULTS AND DISCUSSION

Synthesis and characterization of tetranuclear Ru(II) arene complexes

The hydrazone ligands were easily prepared in good yields by the condensation of benzil (**L-1**) and oxalaldehyde (**L-2**) with isoniazid at a 1:2 molar ratio following a previously established protocol, as shown in **Scheme S1** [14]. These ligands were further allowed to react with the ruthenium(II) arene precursor [(η^6-*p*-cymene)$RuCl_2$]$_2$) in a 1:2 molar ratio in the presence of Et_3N as the base at room temperature. This synthetic scheme enables the final tetranuclear arene Ru(II) complexes (i.e., **Ru-1** and **Ru-2**) to be obtained with the common formula [Ru_4(η^6-*p*-cymene)$_4$ (L1-2)$(Cl)_6$] in excellent yields (**Figure 1**).

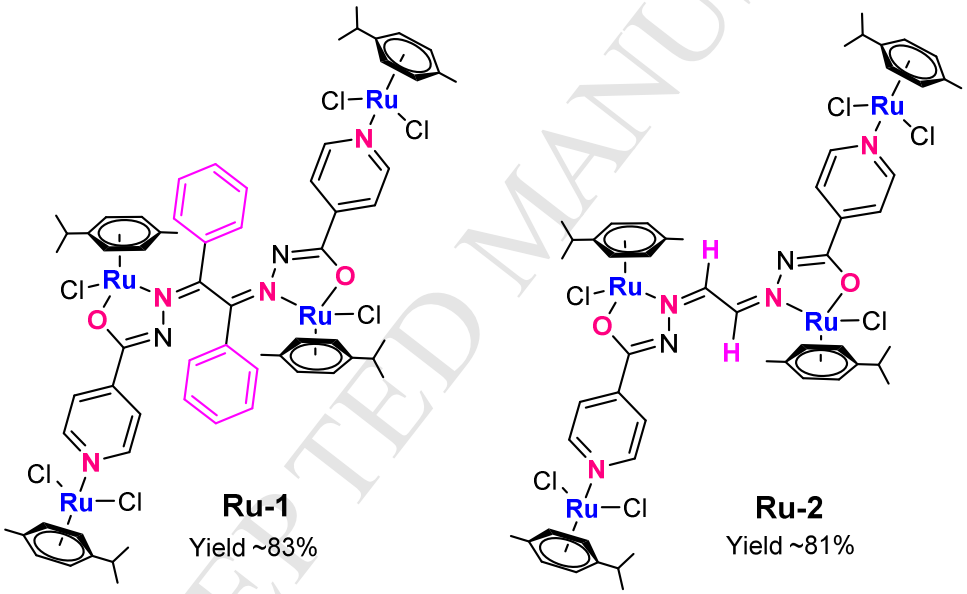

Figure 1. Structures of tetranuclear Ru(II) arene hydrazone complexes.

The Fourier-transform infrared (FT-IR) spectra of the free ligands displayed $\nu_{C=N}$ and $\nu_{C=O}$ stretching vibrations in the region of 1548-1555 cm^{-1} and 1650-1656 cm^{-1}, respectively (**Figure S1**). This suggested that free hydrazone ligands were presented in the amide form in the solid state. However, absorption peaks that are assigned to ν_{N-H} and ν_{C-O} stretching vibrations were not observed in the complexes **Ru-1** and **Ru-2** (**Figure S2**). The coordination of the ligands to the Ru(II) ion through an azomethine nitrogen is expected to reduce the electron density in the azomethine link, which could induce spectral change. We indeed observed such a shift of the vibrational frequency to

1487-1499 cm^{-1} upon ligand complexation, indicating the coordination of azomethine nitrogen to the Ru(II) ion. On the other hand, the absorption bands in the spectral range of 1334-1336 cm^{-1} corresponded to the imidolate oxygen that was expected to coordinate to the Ru(II) metal. Furthermore, the complexes showed the strong bands corresponding to $\nu_{M\text{-}N}$ in the region of 514-523 cm^{-1} (**Figure S2**). Therefore, the FTIR spectra confirmed the mode of coordination of the hydrazone ligand to the ruthenium(II) ion *via* the azomethine nitrogen and imidolate oxygen [18, 32]. Accordingly, the ligands are coordinated to metal *via* imine nitrogen and imidolate oxygen atoms.

Furthermore, we determined the absorption of **Ru-1** and **Ru-2** using a UV-vis spectrophotometer. As depicted in **Figure S3**, **Ru-1** and **Ru-2** exhibited strong absorption at approximately 307-310 nm and 255–257 nm, which correspond to highly intense π–π* and n–π* ligand-centered transitions, respectively. Moreover, the relatively low absorption in the visible region from 479-484 nm could be assigned to MLCT transitions [33]. We then carefully characterized both complexes using ^{1}H and ^{13}C NMR spectra, and the characteristic signals from coordinated *p*-cymene appeared at the expected shifts [34]. The ^{1}H NMR spectra of both complexes were recorded in $CDCl_3$ and are shown in **Figure S4-5**. Multiplets observed in the region of δ 7.09-8.73 ppm were assigned to the aromatic protons of hydrazone ligands in the complexes. In addition, the singlet peaks at 10.8 ppm are due to the presence of the –NH proton in free ligands. The cymene protons appeared in the region of δ 5.83-3.67 ppm. In addition, the methyl group of *p*-cymene appeared as a singlet at approximately δ 2.31–2.34 ppm. Furthermore, the two isopropyl methyl protons of *p*-cymene appeared as two doublets in the region of δ 0.55-1.23 ppm, and the methine protons are present in the region of δ 2.34-2.87 ppm as a septet. Furthermore, the ^{13}C NMR spectra of the complexes are shown in **Figure S6-7**; the signals of the aromatic carbons showed singlet resonances at approximately 112.4-136.4 ppm. The resonance due to C=N and C–O was observed at approximately 165.0 ppm and 174.0 ppm, respectively. The signals observed at 78.6-85.6 ppm and 7.9–102.0 ppm confirmed the presence of the *p*-cymene ligand in the complexes [25]. ESI-MS analysis was performed to validate the final adducts, showing that the peaks at *m/z* 1460.6 and 1305.6 can be assigned to the tetranuclear form of the **Ru-1** and **Ru-2** complexes, respectively (**Figure S8-9**).

After systemic injection, noncovalent interactions between ruthenium complexes with abundant serum proteins will occur, which may cause loss-of-function of the administered drugs.

The formation of new noncovalent species could manifest as a gradual shift in the UV-vis profile [35]. Therefore, to examine this possibility, we monitored the UV-vis spectra of the complexes in Dulbecco's modified Eagle's medium (DMEM) containing 10% fetal bovine serum (FBS) and in phosphate-buffered saline (PBS) containing 10% DMSO [36]. In DMEM with 10% FBS, both the **Ru-1** and **Ru-2** complexes exhibited minimal changes in the UV-vis profiles, indicating negligible associations with serum proteins [37]. In addition, the two complexes remained intact toward hydrolysis in the mixture of DMSO:PBS, manifesting high stability over 72 h at 8 h intervals (**Figure S10**).

***In vitro* cytotoxicity against human cancer cells**

Next, we assessed the *in vitro* cytotoxicity of the **Ru-1** and **Ru-2** complexes against various human cancer cell lines (i.e., A549, A549cisR, MCF-7, LoVo, and HuH-7). After a 72-h incubation of the compounds, the cell viability was determined by the conventional MTT assay. In this experimental setting, cisplatin was also included as a reference. We summarized the values of the half maximal inhibitory concentration (IC_{50}) in **Table 1**. Undoubtedly, we observed the superior activity of using **Ru-1** and **Ru-2** relative to cisplatin in all tested cancer cell lines (**Figure 2**). More interestingly, both complexes **Ru-1** and **Ru-2** showed much lower IC_{50} values in cisplatin-resistant A549cisR cells. For instance, cisplatin displayed an IC_{50} value of 17.24 ± 1.5 μM in A549cisR cells; however, **Ru-1** and **Ru-2** significantly decreased these values to 3.39 ± 0.5 and 5.70 ± 0.3 μM in A549cisR cells, respectively. Several cellular processes can contribute the resistance of cells toward cisplatin, including the decrease in intracellular drug uptake, the enhanced level of thiol-rich proteins (e.g., metallothionein and glutathione), the increased DNA repair, and the tolerance of cell-death pathways [38]. However, we observed potent cytotoxicity of **Ru-1** and **Ru-2** in cisplatin-resistant A549 cells, as evidenced by the drug resistance factor (**Table 1**). Therefore, the complexes presented here hold the potential to overcome drug resistance induced by cisplatin.

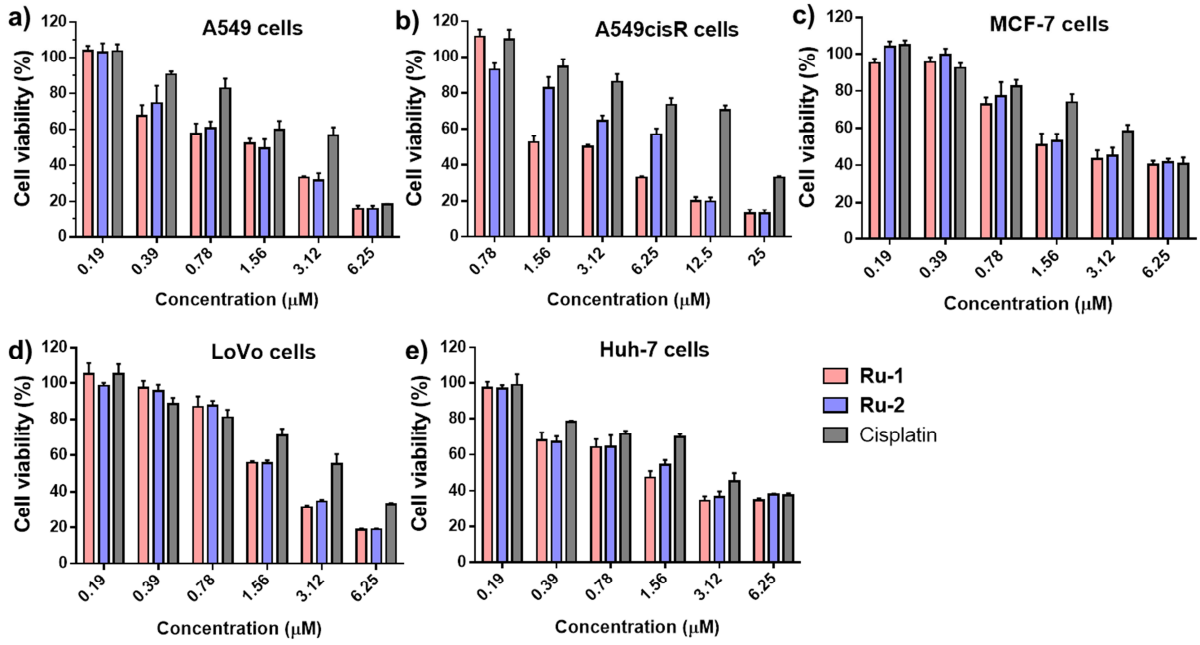

Figure 2. *In vitro* cytotoxicity in (**a**) A549 cells, (**b**) A549cisR cells, (**c**) MCF-7 cells, (**d**) LoVo cells and (**e**) HuH-7 cells after 72-h treatment with **Ru-1**, **Ru-2** and cisplatin.

Table 1. Antitumor potential of Ru(II) arene complexes after 72 h of incubation (expressed as IC_{50}±SD in μM). [a]

Cell line	Type of cancer cell line	**Ru-1 (FI)**[b]	**Ru-2 (FI)**	cisplatin
A549	Lung carcinoma	1.39 ± 0.15 (1.9)	1.41 ± 0.23 (1.9)	2.68 ± 0.16
A549cisR	Lung carcinoma	3.39 ± 0.47 (5.1)	5.70 ± 0.33 (3.0)	17.24 ± 1.52
[c]RF		2.43	4.04	6.43
MCF-7	Breast adenocarcinoma	2.63 ± 0.30 (1.6)	2.91 ± 0.35 (1.4)	4.24 ± 0.28
LoVo	Colon adenocarcinoma	2.04 ± 0.10 (1.7)	2.09 ± 0.77 (1.6)	3.45 ± 0.27
HuH-7	Hepato cellular carcinoma	1.71 ± 0.20 (1.8)	1.98 ± 0.30 (1.5)	3.04 ± 0.29
RAW 264.7	Murine macrophage cells	10.47 ± 1.18 (0.70)	7.91 ± 1.50 (0.92)	7.30 ± 1.20
HUVEC	Human umbilical vein endothelial cells	6.16 ± 0.26 (0.80)	5.89 ± 0.18 (0.83)	4.90 ± 0.4.3
[d] log $P_{o/w}$		-0.68	0.53	--

[a] Determined by MTT assay. IC_{50} values indicate the molar concentrations of whole Ru(II) complexes **Ru-1** and **Ru-2**, and cisplatin required to inhibit 50% of cell growth with respect to control groups. The data obtained are based on the average of three independent experiments, and the reported errors are the corresponding standard deviations.

[b] FI (fold increase) is defined as IC_{50} (cisplatin)/IC_{50} (**Ru-1** or **Ru-2**).

[c] RF (resistant factor) is defined as IC_{50} in A549cisR/IC_{50} in A549.

[d] The log $P_{o/w}$ values determined *via* the shake-flask method against n-octanol/water (1:1, v/v) partition.

Drug selectivity in killing cancer cells over noncancerous cells

One of the major limitations of existing antitumor drugs is their poor selectivity for killing cancer cells over noncancerous cells, which usually causes side effects and impairs the dose intensification of drugs in clinic. To assess whether **Ru-1** and **Ru-2** exert the activity as cancer-selective agents, we additionally tested the cytotoxicity in noncancerous cell lines including murine macrophage RAW 264.7 and human umbilical vein endothelial HUVEC cells. Cisplatin exhibited the high cytotoxicity in both cells; the IC_{50} values in noncancerous cells are comparable with those in cancer cells (**Table 1 and Figure S11**). Interestingly, the complexes **Ru-1** and **Ru-2** were less toxic than cisplatin in both tested RAW 264.7 and HUVEC cells.

The selectivity index (SI) for each complex can be defined as the ratio of the IC_{50} value in noncancerous cells to the IC_{50} value in cancer cells and is summarized in **Figure 3**. The cytotoxicity difference between cancer cells over noncancerous cells was higher of using the Ru(II) complexes than that of using cisplatin. In particular, **Ru-1** demonstrated the superior selectivity for killing cancer cells over noncancerous cells (**Figure 3**). These results thus evidenced the advantages of the complexes **Ru-1** and **Ru-2** as cancer-selective agents, and they should have the potential to reduce the toxicity to healthy cells and organs when considering the *in vivo* use.

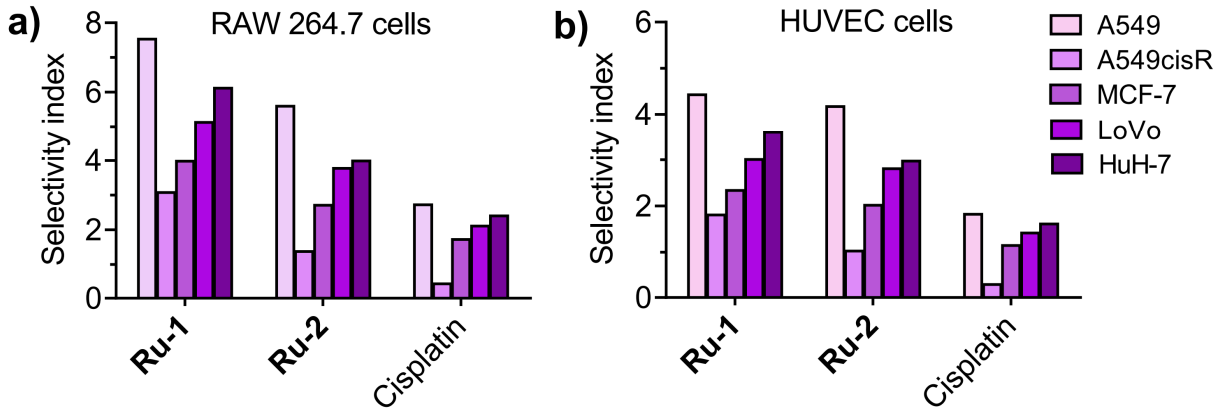

Figure 3. The selectivity index of Ru(II) complexes and cisplatin. The selectivity index is defined as the ratio of the IC_{50} value in RAW 264.7 or HUVEC cells to the IC_{50} value in cancer cells.

The EdU incorporation assay was further performed to evaluate the antiproliferation activity of the **Ru-1** and **Ru-2** complexes in A549 cells after 24 h of treatment (**Figure 4a**). We chose the IC_{20} concentration for this *in vitro* experiment. The results clearly showed that the cisplatin treatment only produced a negligible effect on the proliferation of A549 cells, whereas **Ru-1** and **Ru-2** significantly reduced their activity. The induction of A549 cell apoptosis by **Ru-1**, **Ru-2** and cisplatin was investigated by apoptosis assays using AO/EB staining and fluorescence microscopy. AO is a vital dye that can stain both live and dead cells and shows green fluorescence. EB only stains cells that have lost their membrane integrity and exhibits red fluorescence. Necrotic cells are stained in red but have nuclear morphologies that resemble those of viable cells. Apoptotic cells appear green and exhibit morphological changes, such as cell blebbing and the formation of apoptotic bodies [39]. As shown in **Figure 4c**, untreated A549 cells showed consistently green fluorescence with normal morphologies; however, the A549 cells treated with **Ru-1**, **Ru-2** and cisplatin showed red orange fluorescence with fragmented chromatin and apoptotic bodies under fluorescence microscope observation, suggesting that low concentrations of **Ru-1**, **Ru-2** and cisplatin predominantly induced apoptosis in A549 cells [40].

Lipophilicity plays a vital role in influencing the antitumor activity of a given Ru(II) arene compound. We thus determined the distribution coefficients (log *P*) by employing the "shake-flask" method to correlate the cytotoxicity with this factor. As illustrated in **Figure S12** and **Table 1**, **Ru-1** and **Ru-2** exhibited log $P_{o/w}$ values of -0.68 and 0.53, respectively. The **Ru-1** complex, showing high lipophilicity, may more easily penetrate cell membranes to enhance apoptosis than the **Ru-2** complex [41].

The superior cytotoxic activity of **Ru-1** and **Ru-2** may also be partially attributed to the extended π-π* conjugation of phenyl ring resulting from ligand coordination of the arene Ru(II) ion [42]. Numerous Ru(II) arene complexes have been assessed for their antiproliferative activity [14, 43]. However, complexes bearing hydrazone units with multiple Ru(II) metal centers have not been explored thus far. This lack of study prompted us to further develop novel multinuclear Ru(II) candidates and explore the efficacies for cancer therapy [44]. Gratifyingly, through rationally tailoring four metal active sites, the *in vitro* activities could be further optimized and improved on the basis of the tetranuclear Ru(II) arene scaffold. Moreover, the increased activity and selectivity of these tetrametallic complexes might be attributed to synergistic cooperation

between the four metals and the hydrazone ligands, thereby supporting our design rationale for generating multinuclear Ru(II) candidates. Further, attempts could be made to create new Ru(II) complexes as potential anticancer candidates by incorporating different spacers or altering substituents on the arene moiety.

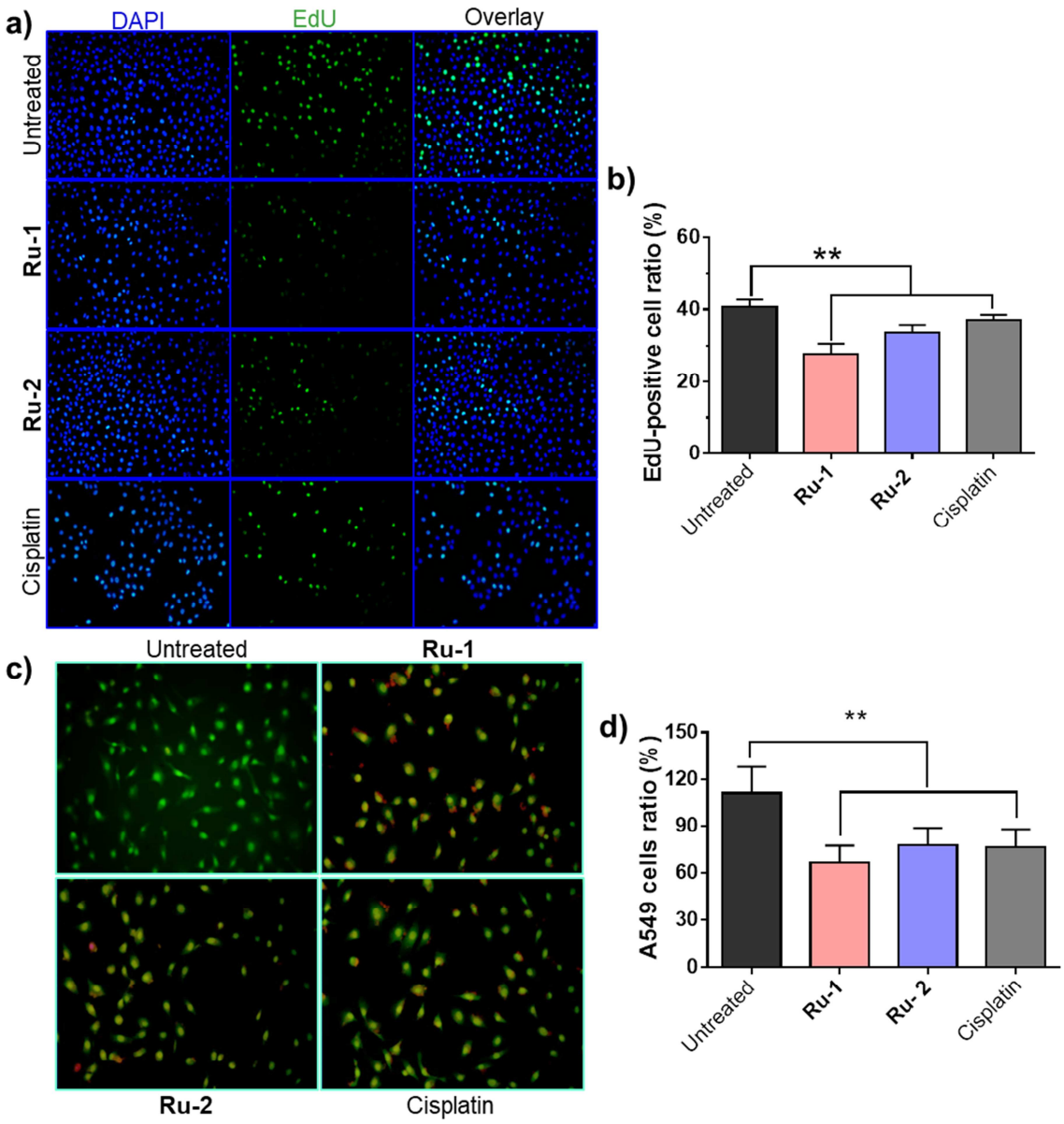

Figure 4. a) A Click-iT EdU assay for determining the proliferation of A549 cells. The cells were treated with **Ru-1** (0.4 µM), **Ru-2** (0.4 µM) and cisplatin (0.9 µM) for 24 h. **b**) Quantification of cell proliferation. The data are presented as the means ± s.d.; n≥5 regions with a total of 1500-2000 cells analyzed; ***p*<0.01. **c**) Dual AO/EB fluorescent staining of A549 cells after treatment with **Ru-1** (0.4

μM), **Ru-2** (0.4 μM) and cisplatin (0.9 μM) for 24 h. **d**) Cell death rates in AO/EB staining were quantified. The data are presented as the means ± s.d.; n≥5 regions with a total of 1500-2000 cells analyzed; ***p*<0.01.

Ru(II) arene complexes induce cancer cell apoptosis

Apoptosis and cell cycle arrest in the cells are the main reasons accounting for the inhibition of cell growth [45]. To examine whether the inhibition of cancer cell growth was a consequence of apoptosis induced by the complexes, we performed an Alexa Fluor 488 Annexin V/propidium iodide (PI) double-staining assay in A549 cells. During apoptosis, phosphatidylserine will be exposed on the outer leaflet of the cell membrane, which can be specifically detected by the binding of fluorescently labeled annexin V [46]. After treatment of the cells (1 μM, **Ru-1**, **Ru-2** and cisplatin) for 24 h, fluorescence-activated cell sorting (FACS) was conducted to analyze the number of apoptotic cells. As shown in **Figure 5a**, the incubation of cells with the complexes induced a high level of apoptosis, and mainly, a late apoptotic event was observed. In addition, compared with cisplatin, **Ru-1** and **Ru-2** were more potent in inducing apoptosis in A549 cells, which was consistent with the MTT assay results [18]. Deregulated cell-cycle control is a fundamental aspect of cancer, and the process is related to the proliferation and death of cancer cells [37]. Therefore, the e□ect of complexes on cell cycle progression was investigated using FACS. As shown in **Figure 5c**, upon exposure of A549 cells to drugs at a 1 μM concentration for 24 h, the percentage of cells in the G0/G1 phase decreased from 67.13% to 28.3%, 24.18%, and 30.5% for **Ru-1**, **Ru-2** and cisplatin, respectively. Notably, **Ru-1** and **Ru-2** elicited a strong S phase arrest in cells, accounting for 68.2% and 73.10% of the cell population, respectively (untreated cells, 21.30%). Thus, the enrichment of the S phase of cancer cells may result in apoptosis by disrupting the cell cycle [47].

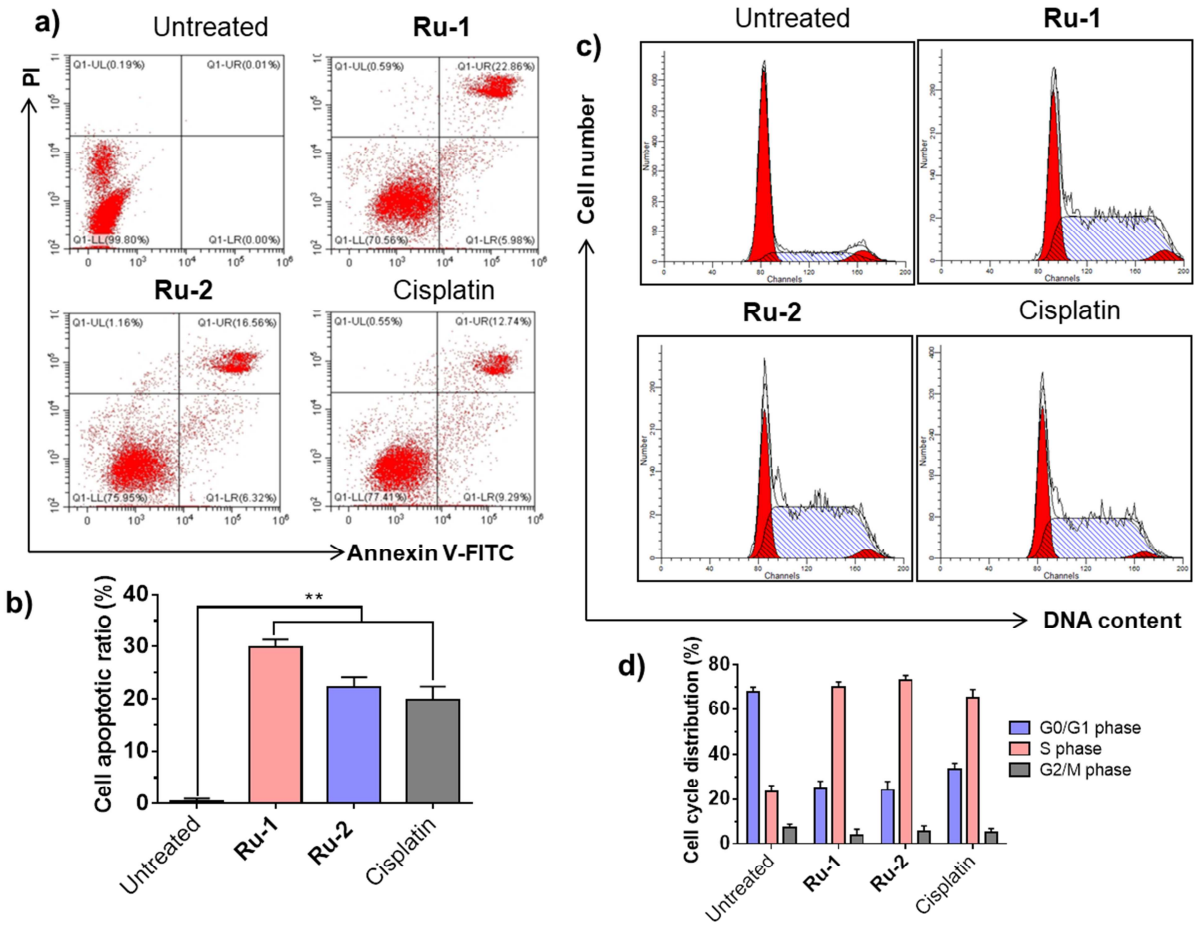

Figure 5. Ru(II) complexes significantly induce apoptosis in A549 cells. The concentrations of **Ru-1**, **Ru-2** and cisplatin used in these studies were 1 μM. (**a-b**) Apoptosis of A549 cells after treatment with compounds was determined by an Alexa Fluor 488 Annexin V/propidium iodide (PI) double-staining assay. The apoptotic ratio is shown in the upper panel, and the quantitative results are shown in the lower panel. (**c-d**) A549 cells were treated with drugs for 24 h, and the cell cycle was analyzed by FACS. The histogram shows the distribution of the cell cycle, indicating that Ru(II) complexes mainly arrested cells at the S phase arrest.

Ru(II) arene complexes inhibit cell invasion and migration

Metastasis and invasion are important incidences in the later period of cancer progression. Therefore, the inhibition of metastasis and invasion is critical for efficient cancer treatment [48]. Cell migration occurs during physiological processes, which play a crucial role in the progression of various diseases, including cancer. *In vitro* migration assays are essential to

understand the mechanism of cell migration and to identify the inhibitory ability of the complexes. The migration is measured by determining the space in the wound closure that is occupied by cells 24 h after treatment (**Figure 6a** and **b**). In A549 cells, migration was significantly reduced after treatment with **Ru-1** and **Ru-2** at 0.4 μM, while cisplatin (0.9 μM) was clearly less active. For example, the ratios of wound closure were 18.8%, 23.3%, and 42.3% for **Ru-1**, **Ru-2**, and cisplatin, respectively [49]. In addition, during the progression of cancer, tumor cells acquire the ability to penetrate the surrounding tissues in a process called invasion. These metastatic cells enter lymphatic or vascular circulation and move through the circulatory system and attach to a new distant location, producing secondary tumors. An effective anticancer drug should be able to impair the movement of cancer cells from the primary sites to other organs in cancer patients. Therefore, the invasiveness of cancer cells was examined by Transwell assay [50]. The invasive A549 cells were seeded on a Matrigel-coated membrane and treated with **Ru-1**, **Ru-2** and cisplatin (0.4, 0.4 and 0.9 μM, respectively) for 24 h. Upon the treatment with the **Ru-1** and **Ru-2** complexes, the numbers of invaded cells were significantly reduced compared to those of the untreated cells (**Figure 6c** and **d**) [51]. Taken together, these results provide evidence that in addition to cytotoxic activity, these tetranuclear Ru(II) complexes have the ability to suppress metastasis and invasion of cancer cells.

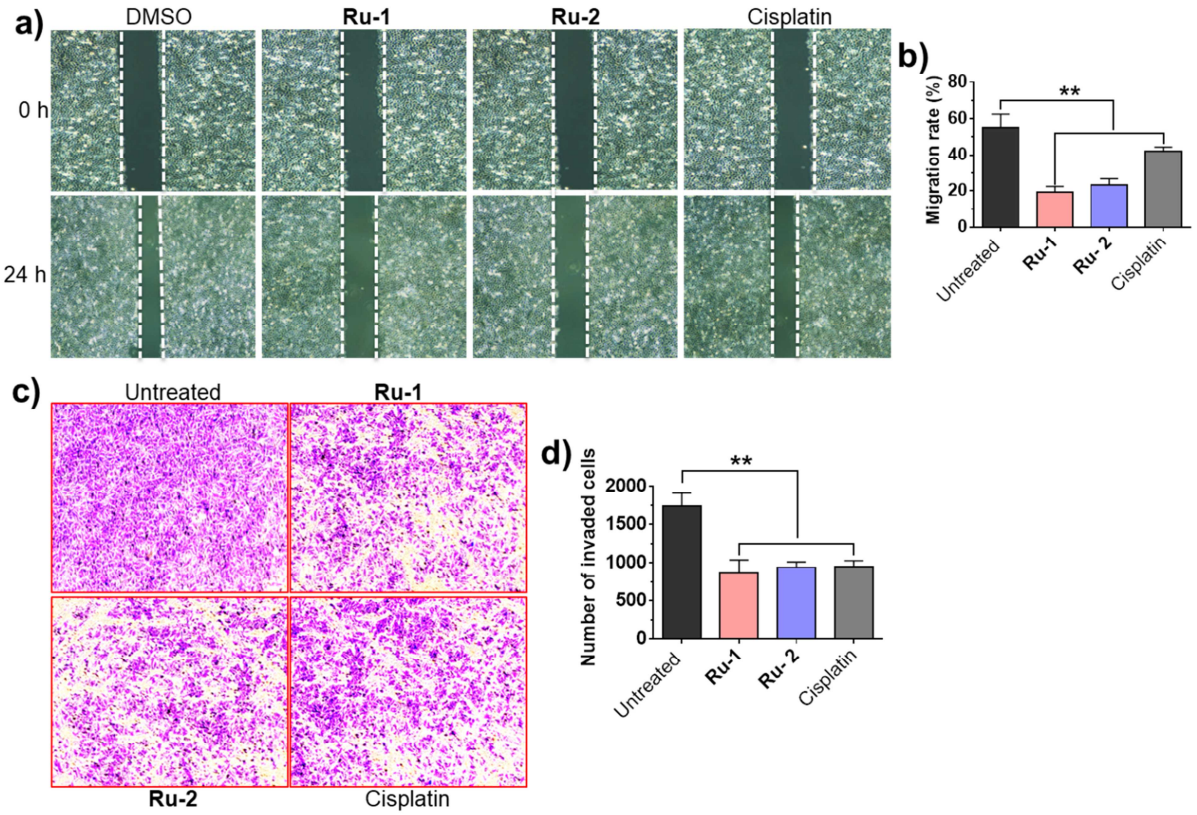

Figure 6. a) The migration of A549 cells was observed by a wound-healing assay. The cells were treated with **Ru-1**, **Ru-2** and cisplatin for 24 h. **b)** Quantification analysis showed that **Ru-1**, **Ru-2** and cisplatin reduced A549 migration. **c)** Invasion of A549 cells was observed by Transwell assay. A549 cells were treated with drugs for 24 h, and the invading cells in the lower chamber were visualized by microscopy. **d**) The number of invading cells upon treatment with drugs was significantly reduced compared with that of the untreated cells.

In vivo systemic toxicity

Finally, to explore the systemic toxicity, a series of animal experiments were carefully conducted. Because of the superior cytotoxicity and antimetastatic activity of **Ru-1** observed in the cell-based results, we chose **Ru-1** as a model compound to evaluate the safety profile in healthy ICR mice. The mice (n = 9, four females and five males in each group) were intraperitoneally injected with **Ru-1** (dissolved in DMSO, 3, 6, 12, 18, and 25 mg/kg) five successive times every other day. For comparisons, saline, the vehicle DMSO and cisplatin administered in its clinical formulation (3, 6, and 12 mg/kg) were injected. The body weights and

survival of the mice were recorded during the period of the study. Unfortunately, all of the mice receiving cisplatin at a dose of 6 mg/kg died, whereas the survival rate in **Ru-1**-treated mice (6 mg/kg) was 100% (**Figure 7**), and the body weight remained stable (**Figure S13**). We further intensified the doses of the **Ru-1** complex in animals and found that seven out of nine mice could tolerate the dose of 12 mg/kg. The LD_{50} values were estimated on the basis of the threshold at which the body weight loss exceeded 20%. Impressively, the LD_{50} value of **Ru-1** (18.1 mg/kg, 95% LD_{50}, 13.9-25.8 mg/kg) was at least 6-fold higher than that of cisplatin (less than 3 mg/kg).

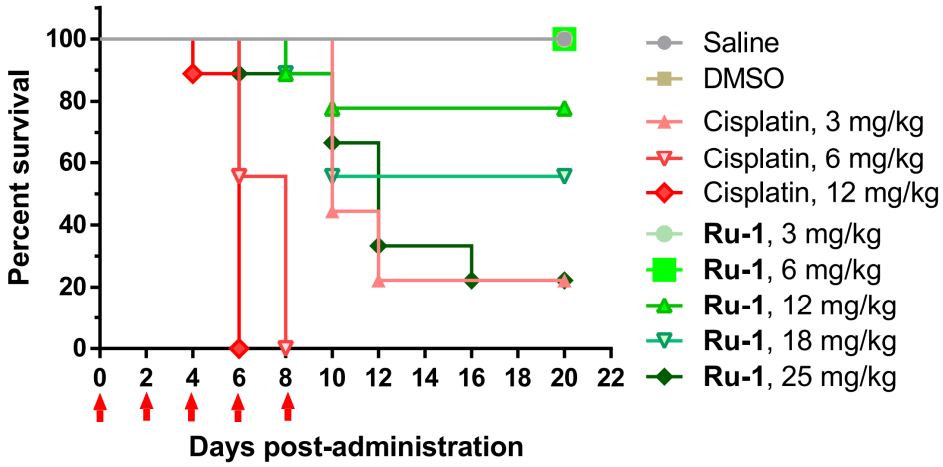

Figure 7. Survival of healthy ICR mice following intraperitoneal injection of saline, DMSO, cisplatin and **Ru-1** for five successive times every other day. The mice were defined as dead when the body weight loss exceeded 20%. Arrows indicate the intraperitoneal injections.

Prior studies showed that cisplatin could lead to serious symptoms such as hyperemia, edema, and inflammatory infiltration of the kidney, accompanied by hydropic or ballooning degeneration of proximal tubular epithelial cells, cytoplasmic relaxation, and exudates from glomerular capsules [52, 53]. Thus, we performed histological analyses to examine the damage of the drugs to major organs. Representative images using hematoxylin-eosin (H&E) staining are shown in **Figure 8** and **Figure S10**. The results revealed a mass of vacuolization (i.e., accumulation of white vesicles) in the cell cytoplasm of renal tubules in the cisplatin-treated mice, which indicated high cisplatin-induced renal damage. Fortunately, no damage was observed in major organs, including the kidney, in the mice receiving **Ru-1** (6 mg/kg), showing similar histological characteristics as those of saline-treated mice. More encouragingly,

administration of **Ru-1** at high doses of up to 12 mg/kg also did not cause obvious damage to these organs (**Figure S10**).

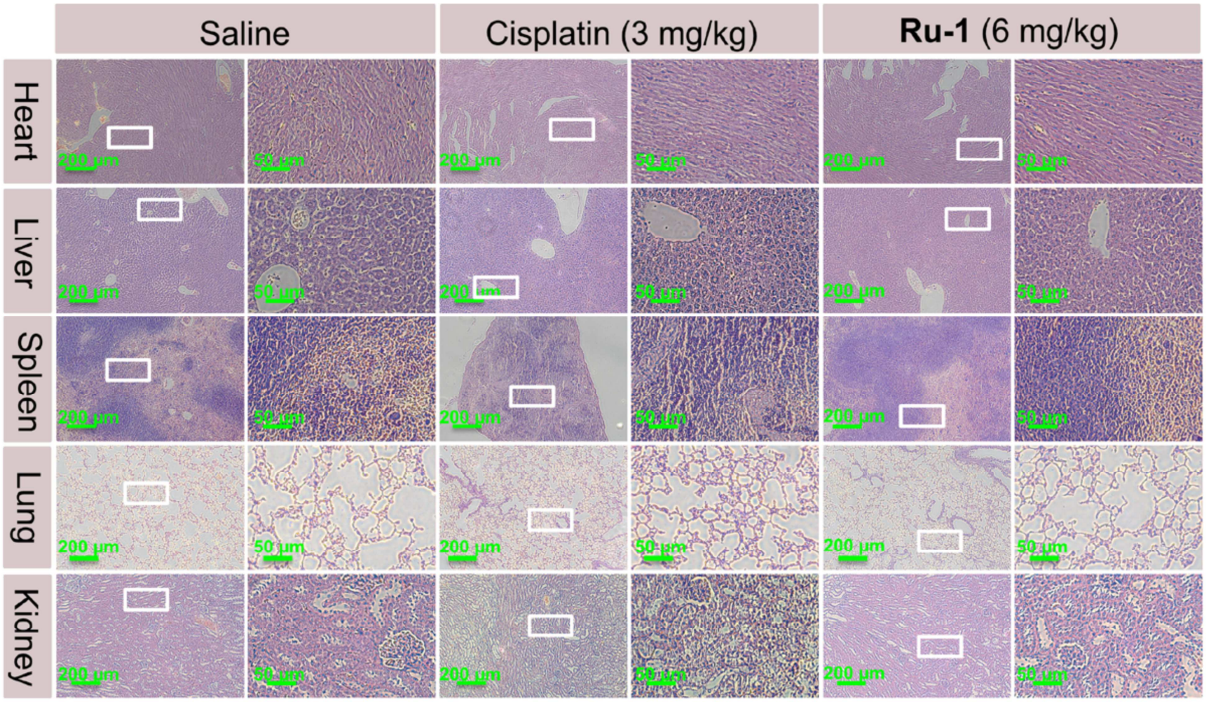

Figure 8. H&E stained tissue slices of the organs (heart, kidney, liver, lung, and spleen) excised from the mice treated with saline, cisplatin (3 mg/kg) and **Ru-1** (6 mg/kg). The images on the right are the enlargement of the region in the white rectangle.

To further validate the damage of cisplatin and **Ru-1** toward the kidney, we conducted the TUNEL assay. As shown in **Figure 9**, intraperitoneal injection of cisplatin resulted in extensive apoptosis in kidney sections, which was well correlated with the H&E results. Conversely, negligible nephrotoxicity in the mice administered **Ru-1** at a dose of 6 mg/kg was observed. Taken together, all results suggest that the compound **Ru-1** exhibits low systemic toxicity and is potentially more tolerated by animals than cisplatin.

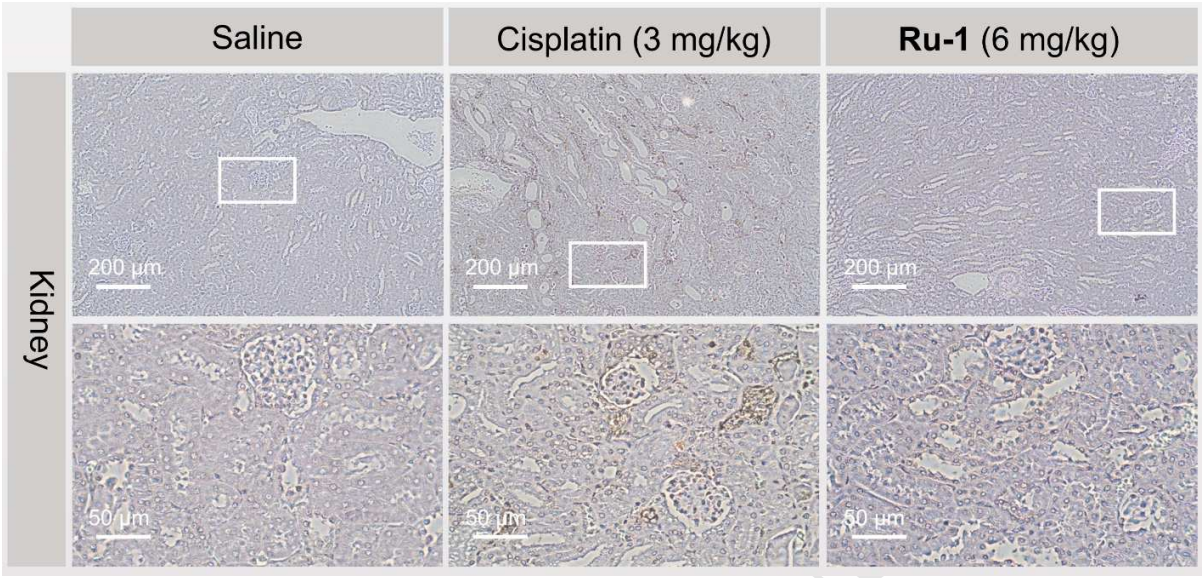

Figure 9. Representative TUNEL analysis of the excised kidneys from the mice treated with saline, cisplatin and **Ru-1** complexes. The images on the second line are the enlargement of the region in the white rectangle. Obviously, potent induction of apoptosis was observed in the kidneys of the mice receiving cisplatin (3 mg/kg) but not in the kidneys of the mice receiving **Ru-1** (6 mg/kg).

3. CONCLUSION

In conclusion, two novel tetranuclear Ru(II) arene complexes (**Ru-1** and **Ru-2**) have been synthesized and examined for their *in vitro* activity against human cancer cell lines. The complexes, especially **Ru-1**, exhibited higher cytotoxic potency relative to cisplatin by efficaciously inducing cell apoptosis. In addition, the complexes showed antimetastatic activity, reducing the invasiveness of cancer cells. Finally, *in vivo* toxicity studies suggested a remarkable alleviation of systemic toxicity using the **Ru-1** complex compared with cisplatin. Given the intrinsic feature of **Ru-1** in circumventing cisplatin resistance and in showing negligible nephrotoxicity, these Ru(II) arene complexes should find potential use in patients with impaired renal function and deserve further investigation.

4. Experimental section

Materials and methods for the synthesis of tetranuclear Ru(II) arene complexes

$[(\eta^6\text{-}p\text{-cym})RuCl_2]_2$ was purchased from Sigma-Aldrich (Shanghai, China). Benzil, oxalaldehyde and isoniazid were purchased from TCI (Shanghai, China). All other compounds and solvents were purchased from J&K Chemical (Shanghai, China). All reactions were performed in a dry atmosphere. Thin-layer chromatography (TLC) was performed on silica gel 60 F254 precoated aluminum sheets (Merck) and visualized by fluorescence quenching. Chromatographic purification was accomplished using flash column chromatography on silica gel (neutral, Qingdao Haiyang Chemical Co., Ltd). The Fourier-transform infrared (FT-IR) spectra of the samples were recorded on an Avatar370 IR spectrophotometer (Thermo Nicolet, USA) using pressed KBr discs. ^1H and ^{13}C NMR spectra were recorded in DMSO or $CDCl_3$ on a Bruker 400 spectrometer and calibrated to the residual solvent peak or tetramethylsilane (= 0 ppm). Multiplicities are abbreviated as follows: s = singlet, d = doublet, m = multiplet. Mass spectrometry ESI-MS was recorded on an AB Triple TOF 5600+System (AB SCIEX, Framingham, USA). The theoretical calculations were performed using IsoPro software [54]. Reverse-phase high-performance liquid chromatography (RP-HPLC) measurements were carried out on a Shimadzu LC 20 system.

Preparation of benzil isoniazid ligands

A mixture of isoniazid (10 mmol) and benzil and oxalaldehyde (5 mmol) in ethanol (20 mL) containing a drop of conc. HCl was refluxed for 30 min [55, 56]. The white solid formed was collected by filtration, washed with ethanol and diethyl ether and dried *in vacuo*. Yield: 75–90%. NMR data are shown in **Figure S14-15**.

Synthesis of tetranuclear Ru(II) arene isoniazid complexes

A mixture containing $[(\eta^6\text{-}p\text{-cym})RuCl_2]_2$ (10 mmol), isoniazid ligands (10 mmol) and Et_3N (0.2 ml) in 1:1 equivalent of benzene (20 ml) was stirred at room temperature for 6 h. The orange precipitate obtained was filtered, washed with hexane and dried *in vacuo*. The progress of the reaction was monitored *via* TLC.

$[Ru_4(\eta^6\text{-}p\text{-cymene})_4(L\text{-}1)(Cl)_6]$ (**Ru-1**)

FT-IR (KBr): $\tilde{\nu}$ = 1499.1, 1334.3, 523.0 cm^{-1}. UV-Vis (CH_3CN, λ_{max}/nm) (ε_{max}/dm^3 mol^{-1} cm^{-1}): 484 (1581), 310 (4982), 258 (8768). ESI-MS (+ve mode): *m/z* 1460.6 $[M + H - 4Cl]^+$ (calcd *m/z* 1459.1). ^1H NMR (400 MHz, DMSO) δ (ppm): 7.09–8.72 (m, 18H, Ar), 5.78-5.83 (m, 4H, *p*-cym-H), 5.01-5.66 (m, 8H, *p*-cym-H), 3.67-4.02 (m, 4H, *p*-cym-H), 2.80-2.87 (m, 2H, *p*-cym $CH(CH_3)_2$), 2.39-2.46 (m, 2H, *p*-cym $CH(CH_3)_2$), 1.99-2.09 (s, 12H, *p*-cym CCH_3), 1.16-1.23 (m, 6H, *p*-cym $CH(CH_3)_2$), 0.55-1.23 (m, 6H, *p*-cym $CH(CH_3)_2$). $^{13}C\{^1H\}$ NMR (100 MHz, $CDCl_3$, δ, ppm): 8.8, 18.5, 18.9, 21.5, 22.2, 22.6, 29.6, 30.8, 30.9, 79.6, 80.5, 80.7, 81.5, 82.2, 83.0, 85.6, 99.3, 100.6, 101.3, 102.0, 127.8, 128.1, 128.4, 128.5, 128.9, 129.0, 129.8, 129.8, 130.0, 130.1, 130.3, 130.5, 131.7, 133.9, 134.6, 135.8, 136.3, 136.4, 165.1, 166.4, 173.1, 174.0, 193.5. Anal. Calc. for $C_{66}H_{74}Cl_6N_6O_2Ru_4$: C, 49.53; H, 4.66; N, 5.25%. Found: C, 50.06; H, 4.47; N, 5.13%. Orange solid. Yield = 0.427 g (83%). HPLC (1:9 ACN/ H_2O as mobile phase) (% purity): ≥95 % at 220 nm; R_T - 3.24 min.

$[Ru_4(\eta^6\text{-}p\text{-cymene})_4(L\text{-}2)(Cl)_6]$ (**Ru-2**)

FT-IR (KBr): $\tilde{\nu}$ = 1487.8, 1336.8, 514.7 cm^{-1}. UV-Vis (CH_3CN, λ_{max}/nm) (ε_{max}/dm^3 mol^{-1} cm^{-1}): 479 (1212), 362 (2966), 307 (3133), 257 (5536). ESI-MS (-ve mode): *m/z* 1305.6 $[M - H - 4Cl]^+$ (calcd *m/z* 1306.3). ^1H NMR (400 MHz, DMSO) δ (ppm): 7.49–8.73 (m, 8H, Ar), 5.83-5.77 (m, 8H, *p*-cym-H), 5.14-5.32 (d, 4H, *p*-cym-H), 3.67-4.60 (d, 4H, *p*-cym-H), 3.02 (s, 6H, CH_3), 2.79-2.86 (m, 2H, *p*-cym $CH(CH_3)_2$), 2.34-2.50 (m, 2H, *p*-cym $CH(CH_3)_2$), 2.08 (s, 6H, *p*-cym CCH_3), 2.0 (s, 6H, *p*-cym CCH_3), 1.18-1.20 (d, 12H, *p*-cym $CH(CH_3)_2$), 0.98-1.02 (d, 12H, *p*-cym $CH(CH_3)_2$). $^{13}C\{^1H\}$ NMR (100 MHz, $CDCl_3$, δ, ppm): 7.9, 17.81, 20.9, 21.5, 45.2, 54.6, 78.8, 81.6, 82.7, 84.3, 98.1, 100.5, 112.4, 125.1, 127.7, 129.3, 129.7, 135.5, 160.6, 165.1, 174.1. Anal. Calc. for $C_{54}H_{66}Cl_6N_6O_2Ru_4$: C, 44.71; H, 4.59; N, 5.80%. Found: C, 45.01; H, 4.77; N, 5.99%. Red-orange solid. Yield = 0.303 g (81%). HPLC (1:9 ACN/ H_2O as mobile phase) (% purity): ≥95 % at 220 nm; R_T - 3.24 min.

The assessment of stability using UV–Vis spectroscopy

The complexes **Ru-1** and **Ru-2** were dissolved in phosphate-buffered saline (PBS) containing 10% DMSO and DMEM containing 10% FBS (without phenol red) at a final concentration of 50

μM. The absorption of the samples was monitored by UV–Vis spectroscopy over 24 h at 4 h intervals.

Determination of Log *P*

Log $P_{o/w}$ values of **Ru-1** and **Ru-2** were determined using the shake-flask method. The complexes were dissolved in water that was presaturated with *n*-octanol (for 24 h and left to stand until phase separation occurred). The UV–Vis spectrum for each sample was obtained, and the absorbances at the λ_{max} of each compound were determined. Equal volumes of *n*-octanol were added to each sample solution, and the heterogeneous mixtures were shaken for 2 h before centrifuging at 4000 rpm for 1 min to achieve phase separation. The final absorbance of the aqueous phase at the λ_{max} of each compound was determined, and their water–octanol partition coefficient was calculated. All experiments were performed in triplicate.

Cell culture

A549, A549cisR, MCF-7, LoVo, and HuH-7 cells were purchased from the cell bank of the Chinese Academy of Sciences (Shanghai, China). A549, A549cisR and LoVo cells were cultured in RPMI-1640 (Gibco) supplemented with 10% fetal bovine serum (FBS; Gibco). MCF-7 and HuH-7 cells were cultured in Dulbecco's modified Eagle's medium (DMEM) containing 10% FBS and 1% nonessential amino acids. All cells were maintained at 37 °C in 5% CO_2.

Cell proliferation study by the EdU test

A549 cells were seeded into flat-bottomed 48-well plates with 2×10^4 cells per well and incubated at 37 °C under a 5% CO_2 atmosphere for 24 h. **Ru-1**, **Ru-2** and cisplatin (0.4, 0.4 and 0.9 μM, respectively) were then added to the cells and incubated for an additional 24 h at 37 °C. DNA synthesis was quantified at the end of the drug treatment using a Click-iT EdU Alexa Fluor 488 Assay Kit (Invitrogen) according to the manufacturer's protocol. Briefly, EdU (5-ethynyl-2′-deoxyuridine) was first added to each well and incubated for 2 h at 37 °C. Then, the cells were fixed for 15 min at room temperature by adding 4% formaldehyde. Next, 0.5% Triton X-100 was added to the cells and incubated for 10 min. Subsequently, azide-labeled Alexa Fluor 488 was added to the cells, and they were incubated for 30 min in the dark. After staining the nuclei with

Hoechst 33342 (Invitrogen) for 15 min, the cells were imaged using fluorescence microscopy (Olympus, IX71).

Acridine orange-ethidium bromide (AO-EB) staining

Dual AO-EB fluorescent staining was used to evaluate cell apoptosis in A549 cells upon treatment with **Ru-1**, **Ru-2** and cisplatin. Briefly, cells were seeded in 24-well plates at a density of 5000 cells/well and incubated at 37 °C for 24 h. **Ru-1**, **Ru-2** and cisplatin (0.4, 0.4 and 0.9 μM, respectively) were incubated with cells. After 24 h of incubation, the staining solution (10 μL) containing AO (100 μg/mL) and EB (100 μg/mL) was added to each well (500 μL). Immediately, the cells were visualized using a fluorescence microscope (Olympus, BX-60, Japan), and the percentage of dead cells was quantified in at least three random microscopic fields.

Flow cytometry to determine cell cycle distribution and apoptosis

A549 cells were seeded into 6-well plates, incubated at 37 °C, and allowed to attach for 24 h. Then, fresh media containing 1 μM **Ru-1**, **Ru-2** or cisplatin were added and further incubated for another 24 h. The untreated cells were included as the control. After drug treatment, the cells were centrifuged at 1000 RPM for 5 min and washed with cold PBS. The cells were fixed with 75% ethanol at 4 °C overnight. The cells were then collected and washed twice with PBS. Thereafter, the cells were stained with a solution containing propidium iodide (PI) (50 μg/mL) and incubated in the dark for 30 min. Cell cycle distribution was then analyzed with a BD FACSCanto™ II flow cytometer.

The cell apoptotic rate was determined by flow cytometry analysis with the fluorescein isothiocyanate (FITC) Annexin V Apoptosis Detection Kit (Multi Sciences, China). A549 cells were collected by trypsinization, washed twice and resuspended in 500 μL 1 × binding buffer with 5 μL of FITC Annexin V and 10 μL of PI. After incubation for 15 min, the samples were subjected to analysis by flow cytometry. The results were analyzed with the BD FACS Calibur™ system.

Wound healing assay

A549 cells were grown to 90% confluence in a six-well plate after 24 h at 37 °C. A scratch across the cell monolayer was produced using a sterile 10 μL pipet tip. Following the treatment of cells with **Ru-1, Ru-2** and cisplatin (0.4, 0.4 and 0.9 μM, respectively) or 0.1% DMSO as a control, images of wounds were acquired by optical microscopy at time 0 after scratching and at the end of a 24 h incubation period. To quantify the migration rate, the distance of the initial wound was compared with the distance of the healing wound at 24 h after the scratch by the pipet tip.

Cell invasion assay

Matrigel matrix (BD Biosciences) was placed into Transwell filters (30 μL/well, 8.0 μm PET, Millipore) and allowed to complete gelation for 1 h at 37 °C. A total of 200 μL of RPMI-1640 medium containing 4×10^4 A549 cells was added into the top chambers, and 700 μL of RPMI-1640 medium supplemented with 10% FBS was placed in the bottom chambers. Subsequently, the wells in the top chambers were treated with **Ru-1**, **Ru-2** and cisplatin (0.4, 0.4 and 0.9 μM, respectively) for 24 h at 37 °C. After 24 h of incubation, cotton swabs were used to remove the Matrigel and cells that remained in the top chambers. Next, A549 cells on the bottom surface of the membrane were fixed with methanol for 10 min and stained with 0.5% crystal violet for 15 min. The invading cells on the membrane were washed with distilled water and photographed under an optical microscope. The cells were counted in at least three random microscopic fields (magnification, ×200). The experiments were repeated three times.

Animal experiments

All animal studies were conducted in accordance with the National Institute Guide for the Care and Use of Laboratory Animals. The experimental protocols were approved by the Ethics Committee of the First Affiliated Hospital, Zhejiang University School of Medicine.

***In vivo* toxicity**

Healthy ICR mice (4-5 weeks old) were randomized into 9 groups (n = 9, four females and five males in each group) and intraperitoneally injected with different doses of **Ru-1** solution in

DMSO (50 μL) every three days five times. Saline, DMSO, and cisplatin solution (Hospira Australia Pty Ltd.) were used as controls. Cisplatin was administered at doses of 3, 6, and 12 mg/kg. **Ru-1** was administered at doses of 3, 6, 12, 18, and 25 mg/kg. The body weight changes of mice were monitored.

After receiving two injections of saline, DMSO, cisplatin and **Ru-1**, two mice in each group were randomly selected and sacrificed by CO_2 inhalation. The major organs, such as kidneys, livers, lungs and spleens, were collected and fixed with 4% formaldehyde. Then, the tissues were embedded in paraffin and sectioned into 5-μm-thick slices. These slices were stained with hematoxylin and eosin (H&E, Sigma). For the terminal deoxynucleotidyl transferase-mediated dUTP nick-end labeling (TUNEL) assay, the dewaxed and rehydrated kidney sections were incubated with proteinase K for 15 min at 37 °C, rinsed with PBS twice, and rinsed with the TUNEL In Situ Cell Death Detection Kit according to the manufacturer's protocol (Sigma-Aldrich). The TUNEL-stained cells were counterstained with DAB (DAKO) and visualized by optical microscopy in 10 random fields for each group.

Acknowledgement

This work was supported by the Zhejiang province fund (No. 519000-X81801), the National Natural Science Foundation of China (Nos. 81571799 and 81773193), and the Zhejiang Province Preeminence Youth Fund (LR19H160002).

Conflict of interest

The authors declare no potential conflicts of interest.

References

[1] B. Rosenberg, L. Van Camp, T. Krigas, Inhibition of Cell Division in Escherichia coli by Electrolysis Products from a Platinum Electrode, Nature, 205 (1965) 698.

[2] T.C. Johnstone, K. Suntharalingam, S.J. Lippard, The Next Generation of Platinum Drugs: Targeted Pt(II) Agents, Nanoparticle Delivery, and Pt(IV) Prodrugs, *Chem. Rev*., 116 (2016) 3436-3486.

[3] X. Wang, X. Wang, Z. Guo, Functionalization of Platinum Complexes for Biomedical Applications, *Accounts Chem. Res.*, 48 (2015) 2622-2631.

[4] R.G. van der Hoop, C.J. Vecht, M.E.L. van der Burg, A. Elderson, W. Boogerd, J.J. Heimans, E.P. Vries, J.C. van Houwelingen, F.G.I. Jennekens, W.H. Gispen, J.P. Neijt, Prevention of Cisplatin Neurotoxicity with an ACTH(4–9) Analogue in Patients with Ovarian Cancer, *New Eng. J. Med.*, 322 (1990) 89-94.

[5] X. Yao, K. Panichpisal, N. Kurtzman, K. Nugent, Cisplatin Nephrotoxicity: A Review, *The American J. Med Sci.*, 334 (2007) 115-124.

[6] K.D. Mjos, C. Orvig, Metallodrugs in Medicinal Inorganic Chemistry, *Chem. Rev*., 114 (2014) 4540-4563.

[7] T.W. Hambley, Metal-Based Therapeutics, *Science*, 318 (2007) 1392.

[8] L. Zeng, P. Gupta, Y. Chen, E. Wang, L. Ji, H. Chao, Z.-S. Chen, The development of anticancer ruthenium(ii) complexes: from single molecule compounds to nanomaterials, *Chem. Soc. Rev.*, 46 (2017) 5771-5804.

[9] V. Mannancherril, B. Therrien, Strategies toward the Enhanced Permeability and Retention Effect by Increasing the Molecular Weight of Arene Ruthenium Metallaassemblies, *Inorg. Chem*., 57 (2018) 3626-3633.

[10] S. Thota, D.A. Rodrigues, D.C. Crans, E.J. Barreiro, Ru(II) Compounds: Next-Generation Anticancer Metallotherapeutics?, *J. Med. Chem*., 61 (2018) 5805-5821.

[11] S. Grgurić-Šipka, I. Ivanović, G. Rakić, N. Todorović, N. Gligorijević, S. Radulović, V.B. Arion, B.K. Keppler, Ž.L. Tešić, Ruthenium(II)–arene complexes with functionalized pyridines: Synthesis, characterization and cytotoxic activity, *Eur. J. Med. Chem.*, 45 (2010) 1051-1058.

[12] Y.K. Yan, M. Melchart, A. Habtemariam, P.J. Sadler, Organometallic chemistry, biology and medicine: ruthenium arene anticancer complexes, *Chem. Commun*., (2005) 4764-4776.

[13] K.D. Camm, A. El-Sokkary, A.L. Gott, P.G. Stockley, T. Belyaeva, P.C. McGowan, Synthesis, molecular structure and evaluation of new organometallic ruthenium anticancer agents, *Dalton Trans*., (2009) 10914-10925.

[14] M.S. Mohamed Kasim, S. Sundar, R. Rengan, Synthesis and structure of new binuclear ruthenium(ii) arene benzil bis(benzoylhydrazone) complexes: investigation on antiproliferative activity and apoptosis induction, *Inorg. Chem. Front.*, 5 (2018) 585-596.

[15] L. Ji, W. Zheng, Y. Lin, X. Wang, S. Lü, X. Hao, Q. Luo, X. Li, L. Yang, F. Wang, Novel ruthenium complexes ligated with 4-anilinoquinazoline derivatives: Synthesis, characterisation and preliminary evaluation of biological activity, *Eur. J. Med. Chem.*, 77 (2014) 110-120.

[16] Y. Fu, C. Sanchez-Cano, R. Soni, I. Romero-Canelon, J.M. Hearn, Z. Liu, M. Wills, P.J. Sadler, The contrasting catalytic efficiency and cancer cell antiproliferative activity of stereoselective organoruthenium transfer hydrogenation catalysts, *Dalton Trans.*, 45 (2016) 8367-8378.

[17] A. Gatti, A. Habtemariam, I. Romero-Canelón, J.-I. Song, B. Heer, G.J. Clarkson, D. Rogolino, P.J. Sadler, M. Carcelli, Half-Sandwich Arene Ruthenium(II) and Osmium(II) Thiosemicarbazone Complexes: Solution Behavior and Antiproliferative Activity, *Organometallics*, 37 (2018) 891-899.

[18] M.K.M. Subarkhan, R. Ramesh, Ruthenium(ii) arene complexes containing benzhydrazone ligands: synthesis, structure and antiproliferative activity, *Inorg. Chem. Front.*, 3 (2016) 1245-1255.

[19] M.J. Chow, M. Alfiean, G. Pastorin, C. Gaiddon, W.H. Ang, Apoptosis-independent organoruthenium anticancer complexes that overcome multidrug resistance: self-assembly and phenotypic screening strategies, *Chem. Sci*., 8 (2017) 3641-3649.

[20] J. Torres, F. Sepúlveda, M.C. Carrión, F.A. Jalón, B.R. Manzano, A.M. Rodríguez, A. Zirakzadeh, W. Weissensteiner, A.E. Mucientes, M.A.d.l. Peña, Ruthenium Arene Derivatives of

Chiral Ferrocene-Based P,N or P,O Ligands. Transformation of Chloro–Alcohol into Hydrido–Carbonyl Complexes, *Organometallics,* 30 (2011) 3490-3503.

[21] H.J. Lozano, N. Busto, G. Espino, A. Carbayo, J.M. Leal, J.A. Platts, B. García, Interstrand DNA covalent binding of two dinuclear Ru(ii) complexes. Influence of the extra ring of the bridging ligand on the DNA interaction and cytotoxic activity, *Dalton Trans.,* 46 (2017) 3611-3622.

[22] A. Rodríguez-Bárzano, R.M. Lord, A.M. Basri, R.M. Phillips, A.J. Blacker, P.C. McGowan, Synthesis and anticancer activity evaluation of η5-C5(CH3)4R ruthenium complexes bearing chelating diphosphine ligands, *Dalton Trans.*, 44 (2015) 3265-3270.

[23] C. Chen, S. Ni, Q. Zheng, M. Yu, H. Wang, Synthesis, Structure, Biological Evaluation, and Catalysis of Two Pyrazole-Functionalized NHC–RuII Complexes, *Eur. J. Inorg. Chem.,* 2017 (2017) 616-622.

[24] K. Hruskova, P. Kovarikova, P. Bendova, P. Haskova, E. Mackova, J. Stariat, A. Vavrova, K. Vavrova, T. Simunek, Synthesis and Initial in Vitro Evaluations of Novel Antioxidant Aroylhydrazone Iron Chelators with Increased Stability against Plasma Hydrolysis, *Chem Res Toxicol.,* 24 (2011) 290-302.

[25] A. Karakurt, S. Dalkara, M. Özalp, S. Özbey, E. Kendi, J.P. Stables, Synthesis of some 1-(2-naphthyl)-2-(imidazole-1-yl)ethanone oxime and oxime ether derivatives and their anticonvulsant and antimicrobial activities, *Eur. J. Med. Chem.*, 36 (2001) 421-433.

[26] N.G. Kandile, M.I. Mohamed, H. Zaky, H.M. Mohamed, Novel pyridazine derivatives: Synthesis and antimicrobial activity evaluation, *Eur. J. Med. Chem.*, 44 (2009) 1989-1996.

[27] E. Potůčková, K. Hrušková, J. Bureš, P. Kovaříková, I.A. Špirková, K. Pravdíková, L. Kolbabová, T. Hergeselová, P. Hašková, H. Jansová, M. Macháček, A. Jirkovská, V. Richardson, D.J.R. Lane, D.S. Kalinowski, D.R. Richardson, K. Vávrová, T. Šimůnek, Structure-Activity Relationships of Novel Salicylaldehyde Isonicotinoyl Hydrazone (SIH) Analogs: Iron Chelation, Anti-Oxidant and Cytotoxic Properties, *PLoS One*, 9 (2014) e112059.

[28] Z. Zhou, J. Liu, T.W. Rees, H. Wang, X. Li, H. Chao, P.J. Stang, Heterometallic Ru–Pt metallacycle for two-photon photodynamic therapy, *PNAS*, 115 (2018) 5664.

[29] C. Manzotti, G. Pratesi, E. Menta, R. Di Domenico, E. Cavalletti, H.H. Fiebig, L.R. Kelland, N. Farrell, D. Polizzi, R. Supino, G. Pezzoni, F. Zunino, BBR 3464: A Novel Triplatinum Complex, Exhibiting a Preclinical Profile of Antitumor Efficacy Different from Cisplatin, *Clini. Cancer. Res.*, 6 (2000) 2626.

[30] T.A. Hensing, N.H. Hanna, H.H. Gillenwater, M. Gabriella Camboni, C. Allievi, M.A. Socinski, Phase II study of BBR 3464 as treatment in patients with sensitive or refractory small cell lung cancer, *Anti-Cancer Drugs*, 17 (2006) 697-704.

[31] A. Garci, J.-P. Mbakidi, V. Chaleix, V. Sol, E. Orhan, B. Therrien, Tunable Arene Ruthenium Metallaprisms to Transport, Shield, and Release Porphin in Cancer Cells, *Organometallics*, 34 (2015) 4138-4146.

[32] Y.-C. Huang, J. Haribabu, C.-M. Chien, G. Sabapathi, C.-K. Chou, R. Karvembu, P. Venuvanalingam, W.-M. Ching, M.-L. Tsai, S.C.N. Hsu, Half-sandwich Ru(η6-p-cymene) complexes featuring pyrazole appended ligands: Synthesis, DNA binding and in vitro cytotoxicity, *J. Inorg. Biochem.*, 194 (2019) 74-84.

[33] R. Raveendran, S. Pal, Some trans-chlorobis(triphenylphosphine)ruthenium(II) complexes with N,N,O-donor N-(aroyl)-N′-(picolinylidene)hydrazines, *Polyhedron*, 24 (2005) 57-63.

[34] N. Mohan, M.K. Mohamed Subarkhan, R. Ramesh, Synthesis, antiproliferative activity and apoptosis-promoting effects of arene ruthenium(II) complexes with N, O chelating ligands, *J. Organomet. Chem.*, 859 (2018) 124-131.

[35] M.J. Chow, M.V. Babak, D.Y.Q. Wong, G. Pastorin, C. Gaiddon, W.H. Ang, Structural Determinants of p53-Independence in Anticancer Ruthenium-Arene Schiff-Base Complexes, *Mol. Pharmaceutics*, 13 (2016) 2543-2554.

[36] M.J. Chow, M.V. Babak, K.W. Tan, M.C. Cheong, G. Pastorin, C. Gaiddon, W.H. Ang, Induction of the Endoplasmic Reticulum Stress Pathway by Highly Cytotoxic Organoruthenium Schiff-Base Complexes, *Mol. Pharmaceutics*, 15 (2018) 3020-3031.

[37] A. Kurzwernhart, W. Kandioller, S. Bächler, C. Bartel, S. Martic, M. Buczkowska, G. Mühlgassner, M.A. Jakupec, H.-B. Kraatz, P.J. Bednarski, V.B. Arion, D. Marko, B.K. Keppler, C.G. Hartinger, Structure–Activity Relationships of Targeted RuII(η6-p-Cymene) Anticancer Complexes with Flavonol-Derived Ligands, *J. Med. Chem.*, 55 (2012) 10512-10522.

[38] D. Wang, S.J. Lippard, Cellular processing of platinum anticancer drugs, *Nature Rev. Drug Dis.*, 4 (2005) 307.

[39] K. Liu, P.-c. Liu, R. Liu, X. Wu, Dual AO/EB staining to detect apoptosis in osteosarcoma cells compared with flow cytometry, *Medical science monitor basic res.*, 21 (2015) 15-20.

[40] M. Mohamed Subarkhan, R.N. Prabhu, R. Raj Kumar, R. Ramesh, Antiproliferative activity of cationic and neutral thiosemicarbazone copper(ii) complexes, *RSC Adv.*, 6 (2016) 25082-25093.

[41] J. Li, M. Tian, Z. Tian, S. Zhang, C. Yan, C. Shao, Z. Liu, Half-Sandwich Iridium(III) and Ruthenium(II) Complexes Containing P^P-Chelating Ligands: A New Class of Potent Anticancer Agents with Unusual Redox Features, *Inorg. Chem.*, 57 (2018) 1705-1716.

[42] M. Hanif, S. Meier, A. Nazarov, J. Risse, A. Legin, A. Casini, M. Jakupec, B. Keppler, C. Hartinger, Influence of the π-coordinated arene on the anticancer activity of ruthenium(II) carbohydrate organometallic complexes, *Front. Chem.*, 1 (2013) 27.

[43] G. Lv, L. Guo, L. Qiu, H. Yang, T. Wang, H. Liu, J. Lin, Lipophilicity-dependent ruthenium N-heterocyclic carbene complexes as potential anticancer agents, *Dalton Trans.*, 44 (2015) 7324-7331.

[44] M.-G. Mendoza-Ferri, C.G. Hartinger, R.E. Eichinger, N. Stolyarova, K. Severin, M.A. Jakupec, A.A. Nazarov, B.K. Keppler, Influence of the Spacer Length on the in Vitro Anticancer Activity of Dinuclear Ruthenium−Arene Compounds, *Organometallics*, 27 (2008) 2405-2407.

[45] Q. Du, L. Guo, M. Tian, X. Ge, Y. Yang, X. Jian, Z. Xu, Z. Tian, Z. Liu, Potent Half-Sandwich Iridium(III) and Ruthenium(II) Anticancer Complexes Containing a P^O-Chelated Ligand, *Organometallics*, 37 (2018) 2880-2889.

[46] H. Wang, J. Chen, C. Xu, L. Shi, M. Tayier, J. Zhou, J. Zhang, J. Wu, Z. Ye, T. Fang, W. Han, Cancer Nanomedicines Stabilized by π-π Stacking between Heterodimeric Prodrugs Enable Exceptionally High Drug Loading Capacity and Safer Delivery of Drug Combinations, in: *Theranostics*, 2017, pp. 3638-3652.

[47] H. Wang, L. Zhou, K. Xie, J. Wu, P. Song, H. Xie, L. Zhou, J. Liu, X. Xu, Y. Shen, S. Zheng, Polylactide-tethered prodrugs in polymeric nanoparticles as reliable nanomedicines for the efficient eradication of patient-derived hepatocellular carcinoma, in: *Theranostics*, 2018, pp. 3949-3963.

[48] H. Wang, J. Wu, K. Xie, T. Fang, C. Chen, H. Xie, L. Zhou, S. Zheng, Precise Engineering of Prodrug Cocktails into Single Polymeric Nanoparticles for Combination Cancer Therapy: Extended and Sequentially Controllable Drug Release, *ACS App. Mater. & Interfaces*, 9 (2017) 10567-10576.

[49] L. Ma, X. Lin, C. Li, Z. Xu, C.-Y. Chan, M.-K. Tse, P. Shi, G. Zhu, A Cancer Cell-Selective and Low-Toxic Bifunctional Heterodinuclear Pt(IV)–Ru(II) Anticancer Prodrug, *Inorg. Chem*., 57 (2018) 2917-2924.

[50] A. Albini, Y. Iwamoto, H.K. Kleinman, G.R. Martin, S.A. Aaronson, J.M. Kozlowski, R.N. McEwan, A Rapid in Vitro Assay for Quantitating the Invasive Potential of Tumor Cells, *Cancer Re*s., 47 (1987) 3239.

[51] J. Wang, H. Wang, J. Li, Z. Liu, H. Xie, X. Wei, D. Lu, R. Zhuang, X. Xu, S. Zheng, iRGD-Decorated Polymeric Nanoparticles for the Efficient Delivery of Vandetanib to Hepatocellular Carcinoma: Preparation and in Vitro and in Vivo Evaluation, *ACS App. Mater. & Interfaces*, 8 (2016) 19228-19237.

[52] Z. Pezeshki, A. Khosravi, M. Nekuei, S. Khoshnood, E. Zandi, M. Eslamian, A. Talebi, S.N.-e.-d. Emami, M. Nematbakhsh, Time course of cisplatin-induced nephrotoxicity and hepatotoxicity, *J. Nephropathol*, 6 (2017) 163-167.

[53] T. Fang, Z. Ye, J. Wu, H. Wang, Reprogramming axial ligands facilitates the self-assembly of a platinum(iv) prodrug: overcoming drug resistance and safer in vivo delivery of cisplatin, *Chem. Commun*., 54 (2018) 9167-9170.

[54] J. Fernandez-de-Cossio, Efficient Packing Fourier-Transform Approach for Ultrahigh Resolution Isotopic Distribution Calculations, *Anal. Chem.*, 82 (2010) 1759-1765.

[55] M.K. Mohamed Subarkhan, R. Ramesh, Y. Liu, Synthesis and molecular structure of arene ruthenium(ii) benzhydrazone complexes: impact of substitution at the chelating ligand and arene moiety on antiproliferative activity, *New J. Chem.*, 40 (2016) 9813-9823.

[56] E. López-Torres, F. Zani, M.A. Mendiola, Antimicrobial activity of organotin(IV) complexes with the ligand benzil bis(benzoylhydrazone) and 4,4′-bipyridyl as coligand, *J. Inorg. Biochem.*, 105 (2011) 600-608.

Graphical Abstract

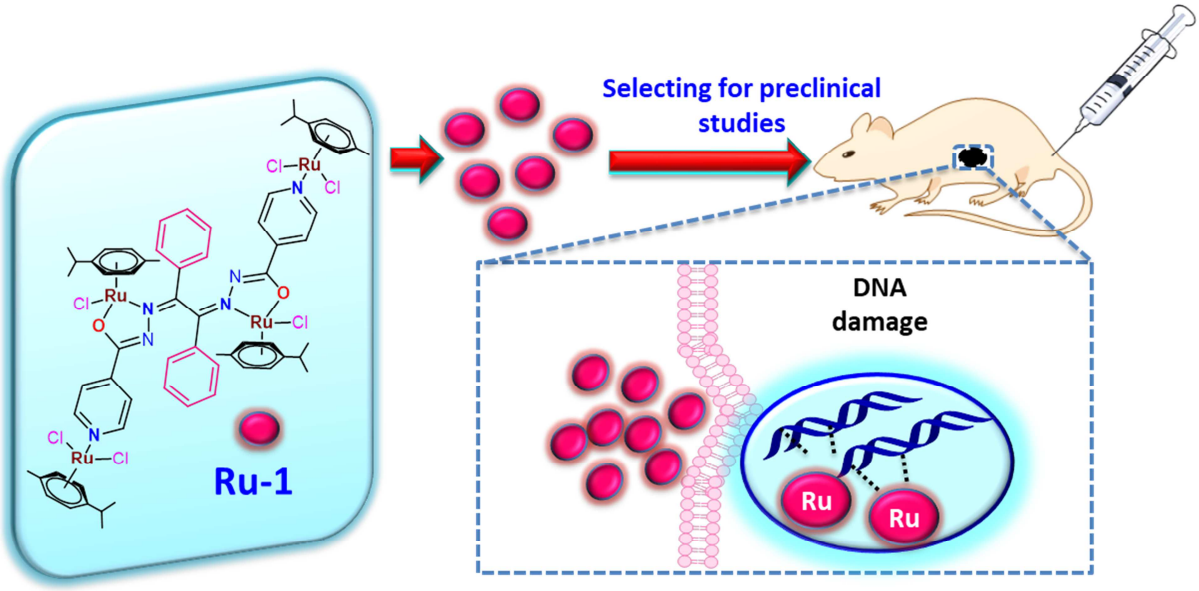

Highlights

- Tetranuclear Ru(II) arene complexes coordinating hydrazone groups were synthesized and characterized by spectral and analytical techniques.
- The **Ru-1** and **Ru-2** complexes displayed higher cytotoxicity than cisplatin in human cancer cell lines.
- The complexes showed antimetastatic activity, reducing the invasiveness of cancer cells.
- Remarkable alleviation of systemic toxicity using the complex **Ru-1** was validated, displaying an enhancement of drug tolerability relative to cisplatin in animals.